

# INVESTIGATIONS OF THE THERMAL STABILITY OF THE MICROSTRUCTURE OF TITANIUM PRODUCED BY INTENSE PLASTIC DEFORMATION

**Yu. R. Kolobov, A. G. Lipnitskii, M. B. Ivanov,  
I. V. Nelasov, and S. S. Manokhin**

*The results of theoretical and experimental studies of the mechanisms of diffusion-controlled processes in nanostructured metals and alloys available in the literature and obtained by the authors are discussed. The molecular dynamic method was used in the context of a modified embedded-atom method was used to investigate the process of collective recrystallization of nanocrystalline titanium. An analytical description of the recrystallization kinetics has been proposed which takes into account the contributions of triple joints to the thermodynamic driving force. Methods of transmission, including high-resolution, electron microscopy were used to examine the kinetics of collective recrystallization in nanostructured titanium VT1-0. The temperature dependence and values of the activation energy for collective recrystallization have been determined. Problems of practical implementation of nanostructured unalloyed titanium in medicine are discussed.*

## INTRODUCTION

Production of new constructional and functional materials with improved properties relies on the results of basic research of the mechanism of formation of their structure and of the nature of the physicochemical processes that occur in materials of this type in actual conditions of their production and use. The physicochemical, electrophysical and other properties of the materials are largely dictated by intercrystalline interfaces (grain boundaries (GBs), subgrains and phases), and also by internal free interfaces related to the presence of pores and cracks) [1–8]. In particular, the lengthening of the boundaries due to a decrease in sizes of grains and phases in going from conventional polycrystalline to submicrocrystalline (SMC) and, especially, to nanocrystalline (NC) and nanostructured (NS) materials results in substantial changes in heat and charge transfer, plastic deformation and fracture, structure degradation and other processes [3, 7, 8]. In the literature, the terms submicrocrystalline and nanocrystalline generally refer to materials whose grain size is 0.1–1 and less than 0.1  $\mu\text{m}$ , respectively. Materials (including composites) produced, as a rule, by using an external action (e.g., intense plastic deformation (IPD)) or by other methods are called nanostructured. The structure elements of materials of this type have even one dimension less than 0.1  $\mu\text{m}$ . For the metal materials produced by IPD methods the structure dispersion is often characterized by the size of grain-subgrain structure elements measured experimentally (e.g., by using transmission or scanning electron microscopy) which generally does not coincide with the spacing between high-angle boundaries, i.e. with the grain size of the polycrystal. Therefore, this factor should be specially discussed when comparing experimental data with predictions of theoretical models of the processes occurring in materials of this type.

In this paper the discussion is focused on the features and mechanisms of the diffusion-controlled processes developing at intercrystalline interfaces in metal systems with SMC structure in the NS state, and also on the

contribution of the mentioned processes to the structure formation and properties. It can be supposed that the science of diffusion-controlled processes occurring at internal interfaces is a research field in which close interaction between experiment, theory, and computer simulation is of principal importance [9]. This is due to a variety of factors that affect the development of the mentioned processes at the atomic level. In the present paper the basic attention is given to the discussion of the results of investigations of the features and mechanisms of diffusion-controlled growth of grains during recrystallization of SMC and NC titanium, which find wider and wider use in traumatology, orthopedy, and stomatology. Original results obtained by the authors and a review of previous studies are presented. The authors do not pretend to give a comprehensive analysis of the problems involved and rely mainly on the results of their own studies. The review is finished by a discussion of the practical implementation of the materials investigated and of the technologies developed largely based on intended harnessing of the revealed features of diffusion-controlled processes.

## **1. FEATURES OF DIFFUSION AND DIFFUSION-CONTROLLED PROCESSES IN NANOSTRUCTURED METAL MATERIALS**

Bulk submicrocrystalline and nanostructured metals, alloys and composites based on them, which are produced by using intense plastic deformation in combination with conventional mechanical and thermal treatments, have been actively developed and studied in the last one and a half decades. According to the accepted terminology, as mentioned above, metals and alloys with grain sizes ranging between 100 and 1000 nm are classified as SMC materials and those with the size of grain-subgrain structure elements less than 100 nm as NS materials. However, in many cases the fraction of nanosized grains (diameter less than 100 nm) in the structure of SMC metals and alloys with the mean grain size being several hundreds of nanometers can make up to several tens of percents. In this case, as shown in many studies [3, 7], the nanosized grains are responsible for unique mechanical, physical and other properties. In this connection, in our opinion, materials which show unique properties related a significant (tens of percents) fraction of nanosized grains can be considered as NS metals and alloys. Interest in SMC and NS materials is primarily conditioned by their physicochemical and mechanical properties that are substantially different from the respective properties of conventional ultra-fine-grained (grain size 1–10  $\mu\text{m}$ ) and, especially, coarse-grained (CG) polycrystals (grain size over 10  $\mu\text{m}$ ). In particular, metals and alloys in a nanostructured state possess high strength with satisfactory and, in some cases, even higher plasticity than in a fine-grained state. They show low-temperature and/or high-strain-rate superplasticity [3, 6, 10–12]. The mentioned properties of SMC and NS metals and alloys open prospects for their wide practical use. At the same time, some fundamental, usually structure-insensitive properties of these materials, such as the elastic modulus, Curie and Debye temperatures, specific heat, etc., are varied [3]. It has been revealed that for SMC and NS metals produced by plastic deformation the grain-boundary diffusion coefficients are several orders of magnitude greater compared to those for individual GBs in bicrystals or GBs in coarse-grained polycrystals [13–19]. The increased diffusion coefficient for the state under discussion makes the structure highly sensitive to the action of the environment. Thus, for instance, the diffusion flows of impurities from the surface into the bulk of SMC and NS metals substantially increase the rates of their creep and deformation until fracture occurs [20, 21]. Thus, the processes of grain-boundary diffusion play the key part in the formation of structure-sensitive properties of materials of this type, and this is related to the great length and high diffusion conductance of their grain boundaries.

However, a commonly accepted view on many problems relevant to the features of diffusion and diffusion-controlled processes in NS and NC materials is not available in the literature. Most of the experiments on direct measuring of diffusion parameters presented in the literature have been performed for NC materials. In particular, a wide spread in experimental data on diffusion coefficients and activation energies for diffusion in metals in the NC and NS states has been revealed. Supposedly, this is related to various technological modes of nanostructure formation, to varied concentrations of uncontrolled impurities, and to other factors. For these and other reasons the features of the physical mechanisms underlying the diffusion-controlled processes in NC materials are still not understood in detail. Till now it is debatable whether the grain-boundary diffusion coefficients for NC metals and alloys are different from those for coarse-grained metals or the features of the diffusion-controlled processes in an NC state are related only to a greater portion of grain-boundary matter compared to that in conventional materials [3].

A problem in comparing the results of investigations of the grain-boundary diffusion in NS and NC metals and alloys mentioned by different authors is grain-boundary porosity, which is often detected in materials produced by using intense plastic deformation [22–24]. The porosity can be responsible for ultra-high-rate diffusion along free surfaces of grain-boundary pores and cracks. With this mass transfer mechanism the effective values of measured diffusion coefficients can be many orders of magnitude greater than the corresponding values for grain-boundary diffusion in coarse-grained polycrystals.

However, it can be supposed that the probability of the pore formation depends on the mode and conditions of realization of intense plastic deformation. With participation of the authors of this paper it has been shown that, for instance, the formation of SMC and NC structures due to intense plastic deformation realized by the method of transverse-screw rolling in conical rollers in an optimum deformation mode does not give rise even nanoporosity [26, 27].

To improve the operating characteristics and estimate the lifetime of NC and NS materials under actual service conditions calls for solving the problem of thermal stability of the nanostructured state and developing methods for inhibiting recovery and recrystallization processes. The reduced temperature of the onset of these processes and their high-rate development in the state under consideration are due to the high excess energy related, as mentioned above, to the developed internal surface of grain boundaries, which are nonequilibrium defects in a polycrystalline material and possess higher energy in comparison with the grain bulk. Traditionally this problem is considered in the context of elucidating the part played by the energy and mobility of grain boundaries in the presence of grain-boundary segregates or finely dispersed second phases in the bulk and at the boundaries of grains [1, 3, 28]. As a result of numerous investigations two basic mechanisms of the inhibition of grain growth have been revealed: a decrease in mobility of GBs due to their interaction with particles of dispersed phases and impurity atoms and a decrease in energy of grain boundaries (and, hence, in the force driving the growth of grains) upon segregation of low-soluble impurities on them. At the same time, the effect of so-called "return" growth kinetics has been found out, such that the growth rate decreases (compared to that estimated from interpolated values for a coarse-crystal state) with the mean grain size being below some critical value [29]. The nature of this effect is yet far from being completely understood. Here it should also be noted that the contribution of triple joints (TJs) of grains is commonly neglected in considering the effects related to the excess energy of the nanocrystalline state. Conflicting data on the energy of triple joints are reported in the publications of many authors. It can be supposed that the discrepancy in data can be accounted for by the use of different models to describe the structure of GBs and TJs [30, 31].

In view of the preceding, to develop and implement in practice optimum modes of nanostructurization of various materials, production of nanocomposites, and analysis of the features of degradation of their structure under actual operating conditions, it is of great importance to understand the mechanisms of diffusion-controlled processes in materials of this type. Experimental investigations on this line are difficult in view of the small size of structure elements and of the atomic scale of the processes involved. The same circumstance necessitates the study of the mechanisms of diffusion-controlled processes in NC materials by methods of computer simulation at the atomic level [16]. Investigations at this level form a basis for developing models which would allow one to predict the behaviour of NC materials by using the methodology of multiscale simulation of materials and processes [9] in combination with methods of mesomechanics [32]. These approaches also allow one to test the models by using computer experimentation. The recent experimental and theoretical investigations of the structure and properties of nanomaterials and of the mechanisms of the physicochemical processes occurring in them strongly suggest that computer simulation is extremely urgent in carrying out basic research and, especially, in developing NC materials [9, 16, 32].

Most of the well-known methods of formation of SMC and NC states by intense plastic deformation [3, 33] are low-output and they considerably increase the material cost. In this connection the perfection of the high-efficiency and low-cost technology of production of an industrial assortment of semifinished SMC and NS titanium and titanium-base alloys with improved mechanical and functional characteristics, developed with participation of the authors of this paper, for using this technology in industrial manufacturing of medical-purpose products with the use of the above-mentioned method of transverse-screw rolling [26, 27, 34] is an urgent task.

Such technology, including, as mentioned, transverse-screw rolling, has been developed and mastered on a small enterprise "Metal-Deform" of Belgorod National Research State University in the framework of a recent complex project "Development of experimental-industrial technologies for production of a new generation of medical

implants based on titanium alloys” of Ministry of Education and Science on the priority line “Nanoindustry and Nanomaterials”. Batch production of structural shapes and plates from commercially pure titanium (alloy VT1-0 and Grade-4) with SMC structure has been run in. Batches of implants for traumatology (plates and screws) are produced from this material on the production basis of one of the project executors (State Unitary Enterprise “All-Russia Research and Design Institute of Medical Tools”, Kazan). These products have successfully passed clinical trials, have been certificated, and now they are delivered to clinics of the Russian Federation.

It is well-known that semifinished submicrocrystalline materials produced by intense plastic deformation feature high internal stresses whose sources are strain-induced grain boundaries, dislocations, and dislocation subboundaries. These stresses make the production of articles laborous and can result in warpage, which may hinder their subsequent use. The simplest way of relieving internal stresses in a metal semifinished item is its heating and soaking at a certain temperature. In semifinished items produced from SMC titanium VT1-0, Grade-4 the residual stresses are reduced to a safe level (with high mechanical properties retained) by pre-recrystallization annealing after the cycle of their technological revision. It is supposed that this opportunity can be realized due to the formation of finely dispersed segregates, which block the migration of grain boundaries and thus inhibit recrystallization [3, 35, 36]. However, this problem demands a special discussion, which will be presented in the next sections.

## **2. MOLECULAR DYNAMIC SIMULATION OF THE RECRYSTALLIZATION OF NANOCRYSTALLINE TITANIUM**

Nanocrystalline materials with the mean grain size less than 100 nm are of great practical interest owing to a unique combination of their physical and mechanical properties [36–38]. By present time several methods of production of these materials have been developed: nanopowder compaction [39], partial crystallization from an amorphous state [40], and primary recrystallization of highly strained materials where numerous nuclei of new grains are formed [41]. Irrespective of the production method, the material features a great fraction of atoms located in intergrain regions. As the contribution of grain boundaries to the excess energy of a polycrystal in relation to its crystalline analog rapidly increases in inverse proportion to the mean grain size, a great thermodynamic force exists in NC materials to reduce the total area of GBs or, which is the same, to increase the mean grain size ( $D$ ). Therefore, as mentioned, one of the most important concerns with practical implementation of NC materials is their thermal stability in relation to the growth of grains. In this connection, significant attention of researchers is given to studying the kinetics of grain growth in the NC state and to the possibility to affect this process with the aim of its partial or complete inhibition at the temperatures of technological processing and practical use of the materials. According to the classical notions developed for polycrystals, the problem of stability of an NC state in relation to an increase in grain size  $D$  is considered in terms of the mobility and energy of grain boundaries. Two basic mechanisms of inhibition of grain growth are known: a decrease in mobility of GBs due to fastening them by dispersed phase particles or the interaction of GBs with inactive impurity atoms and a decrease in GB energy and, hence, in the force driving the grain growth, during grain-boundary segregation of impurity atoms. Many papers and some reviews and books (see [41] and the cited works) are devoted to studying the grain growth in NC materials. The existence of an NC state of alloys which possesses lower energy in comparison with a crystalline state due to a decrease in GB energy resulting from segregation of low-soluble impurities has been predicted theoretically [42]. The experimental and theoretical data on this effect are discussed elsewhere [43, 44]. However, as a whole, the theory of stability of NC states is in the making. Here it should be noted that the structure of NC materials is difficult to describe because of a variety of important factors that may introduce incorrectness in an interpretation of experimental results. These factors are: distortions of the crystal lattice and the related stresses, inhomogeneities of chemical and phase compositions, ordering effects, and other factors inherent in heterogeneous systems [41]. In this connection, to identify the features of the calculations of the thermodynamic force and the kinetics of grain growth in an NC material, it is of interest to perform computer experiments on simulation of the growth of grains by the method of molecular dynamics. These model experiments allow one to investigate the process of grain growth in a perfect monoatomic system disregarding the influence of impurities and to elucidate the effect of the small (tens of nanometers) grain size on the kinetics of grain growth as a basis for further studying of this process in heterogeneous systems. Earlier a molecular dynamic simulation has been

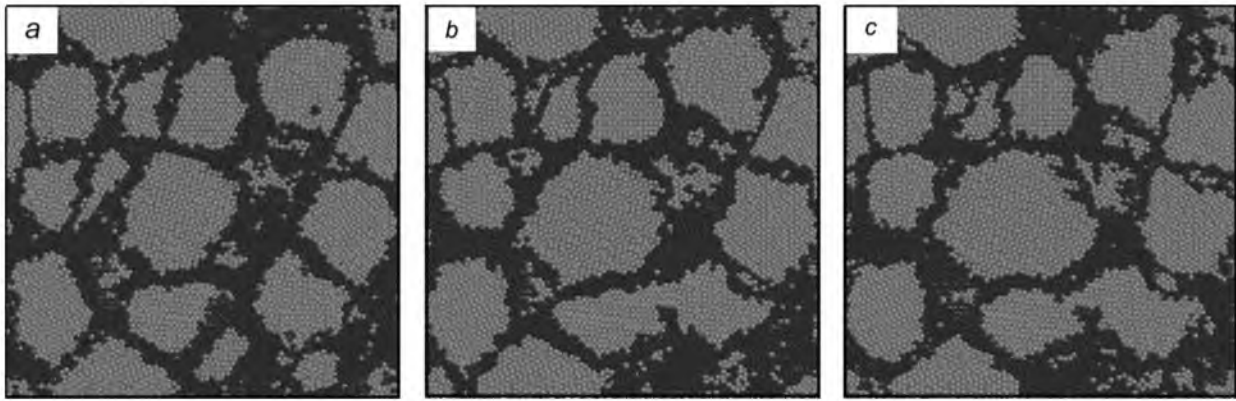


Fig. 1. Section of a model titanium sample containing 416761 atoms in a calculation mesh shaped as a cube  $20 \times 20 \times 20$  nm in size with periodic boundary conditions after molecular-dynamic simulation at 1000 K. The light grey color selects atoms with fcc titanium local environment and the black color selects atoms with other local environment which are preferentially located in grain boundaries and in their triple joints: the initial state containing 100 grains with  $D = 5.1$  nm in a calculation mesh (a), the state at the 150th picosecond (b), and the state at the 300th picosecond ( $D = 6.8$  nm) (c).

performed for titanium with the use of semiempirical atom-atom interaction potentials [45] constructed in the context of the modified embedded atom method. These potentials well reproduce the  $P$ - $T$  phase diagram of titanium that has been obtained from experimental data and results of first-principle calculations by the electron density functional method [46]. We previously used these potentials in studying the self-diffusion that occur over the intergrain region, and in the present paper we can compare the energy of the process of grain growth and the energy of the self-diffusion over the intergrain region for fcc titanium.

Note that in the molecular dynamic investigations of the grain growth in nanocrystalline materials performed to the present time [47] little attention was given to the dependence of the mean grain size on simulation time. It was only qualitatively discussed if the kinetics of grain growth is a linear or a parabolic function [48].

Eleven molecular-dynamic experiments have been performed to simulate nanocrystalline titanium at constant temperatures in the range from 700 to 1200 K with a step of 50 K. To construct model samples, the well-known approach was used which is based on braking the space into Voronoi polyhedrons and filling the polyhedrons with crystal grains which grow from nuclei at the centers of polyhedrons with occasional crystalline orientation of each nucleus. For the fast Verleta algorithm used, the molecular dynamic simulation step was 3 fs. A sample was preliminary "heated" for 2000 steps to a given test temperature by the atomic velocity scaling method and then the Nose-Hoover algorithm was used for 3000 steps [49]. Thereafter a molecular dynamic experiment was performed for 100 000 steps. The total energy of the system averaged over every 100 steps was recorded. The system state was saved for analysis every 10 000 steps. The model sample contained 100 grains, shaped as Voronoi polyhedrons, in a calculation mesh. The initial mean grain size  $D$  determined by the secant method was 5.1 nm. Note that the grain size estimated by this method is related to the often used determination of the mean grain size  $D^*$  as the diameter of a sphere whose volume is equal to the mean volume of grains in the sample by the relation  $D^* = 1.65 D$  [50].

Figure 1 shows an example of a simulated nanocrystalline titanium sample containing 416761 atoms in a calculation mesh and shaped as a cube with periodic boundary conditions after molecular dynamic simulation at 1000 T. At the mesh center a grain is clearly seen which has increased in size during simulation. Below the grain we see how two grains merge into one grain; this is a mechanism of increasing the mean grain size during collective recrystallization of a nanocrystalline material. It can be seen that collective recrystallization without rapid growth of one or several grains took place.

The used method of calculation of the mean grain size during simulation demands special discussion. The direct determination of  $D$  by counting the number of crosses of the secant with grain boundaries, as can be seen from Fig. 1, is problematic because of the complexity of the regions of grain boundaries and triple joints for the mean grain

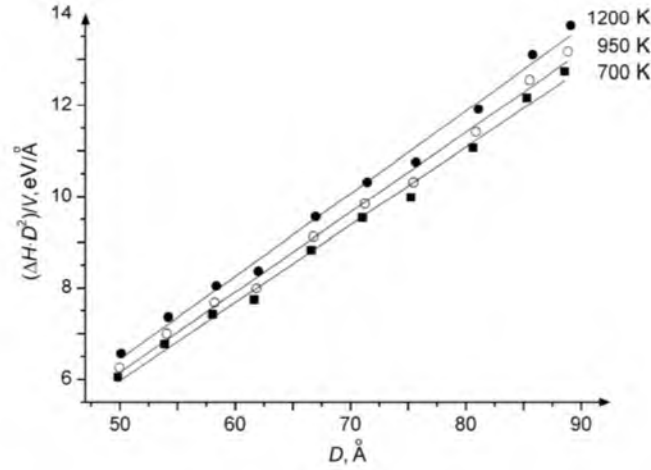


Fig. 2. Calculated excess energy per unit volume, multiplied by the squared mean grain size  $D^2$ , as a function of  $D$ .

sizes under consideration for which the sections of grain boundary regions can hardly be considered thin lines and triple joints neglected. It should be noted that this method is nevertheless used (see, e.g., Ref. 48) despite the mentioned problem with exact determination of  $D$ . In the present work we have obviated this problem by using an exact thermodynamic relation between the excess energy per unit volume and the mean grain size  $D$  in the nanocrystalline material [50].

To associate the obtained energy of the system with the mean grain size, test calculations have been performed for model nanocrystalline titanium samples with known (by construction) mean grain sizes at all test temperatures. To grade the specific excess energy in terms of the mean grain size, the sample temperature was set for 1000 steps by the atomic velocity scaling method and for 1000 steps by using the Nose-Hoover algorithm. Based on the data obtained for the mean energy of the system, the mean energy of grain boundaries and triple joints was determined [50]. The relevant interpolation plots are exemplified in Fig. 2.

The obtained values of the energies of grain boundaries and triple joints were used to associate the mean energy of the system to the mean grain size at a given temperature.

Some results of the molecular dynamic simulation of nanocrystalline titanium at constant temperature for the above-described set of temperatures are plotted in Fig. 3 as relations between the mean grain size and the simulation time. The same plots present the results of interpolation by the analytic relations that have been derived based on consideration of the recrystallization driving force in view of triple joints. These relations are discussed below.

The well-known approach widely presented in the literature is to describe the kinetics of grain growth proceeding from the proportionality of the velocity of migration of the grain boundary,  $v$ , to the effective thermodynamic driving force  $P$  that causes the grain boundary to move [51, 52]:

$$v = M \cdot P, \quad (1)$$

Here  $M$  is the mobility of the grain boundary. The mobility of a grain boundary depends on temperature according to the Arrhenius-type relation

$$M = M_0 \exp\left(-\frac{Q}{k_B T}\right). \quad (2)$$

Here  $Q$  is the activation energy for the grain boundary migration,  $k_B$  is Boltzmann's constant, and  $M_0$  is the preexponential factor.

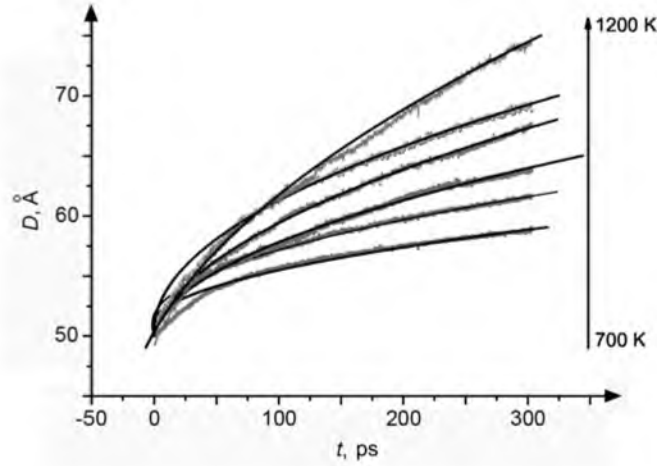


Fig. 3. Mean grain size as a function of the time of isothermal molecular dynamic simulation for nanocrystalline titanium in the temperature range 700–1200 K (temperature step is 100 K). Black symbols show the results of determination of the mean grain size every 0.3 ps of simulation. The lines were drawn according to the interpolation of the grain growth kinetics at constant temperature by the analytic relation discussed in the text.

In the context of the well-known Burke–Tarnball approach [51, 52], it is assumed that the effective thermodynamic driving force for collective recrystallization is the Laplace pressure

$$P = 2\gamma_{\text{GB}} / R, \quad (3)$$

where  $R$  is the mean radius of curvature of the grain boundaries,  $\gamma_{\text{GB}}$  is the mean grain boundary energy per unit area of the grain boundaries in the polycrystalline sample. Using equations (1) and (3) and putting  $v = dR / dt$ , we obtain [52]

$$\frac{dR}{dt} = \frac{\alpha M \gamma_{\text{GB}}}{R}, \quad (4)$$

Integration of this equation yields the relation

$$R^2 - R_0^2 = ct, \quad (5)$$

where  $c = \alpha M \gamma_{\text{GB}}$ ;  $R_0$  is the mean grain radius at  $t = 0$ . Many measurements of the grain size  $D$  as a function of time  $t$  at constant temperature have shown that the grain growth kinetics can be described by the empirical formula [51, 52]

$$D^2 - D_0^2 = c_1 t. \quad (6)$$

The constant  $n$ , as a rule, is not equal to 2. This discrepancy is accounted for by the effect of the grain-boundary segregation of impurity atoms, by the decrease in mobility of grain boundaries, by the formation of inclusions of dispersed phases, and by other factors [52]. We shall not consider these factors and note that, in this case, nanocrystalline titanium is considered in which significant effect of triple joints on excess energy is possible [50]. At the same time, in deriving relation (5) the contribution of triple joints to the driving force responsible for the growth of grains was not considered.

Next we modify relation (5) in view of triple joints. For doing this we note that the effective driving force (3), to within a geometric factor, represents the specific excess energy of a nanocrystalline material per unit volume with triple joints neglected. In view of triple joints, the specific excess energy is given by the equation [50]

$$\frac{dH}{v} = \frac{2\gamma_{GB}}{D} + \frac{\lambda\gamma_{TY}^*}{D^2}. \quad (7)$$

Here  $\Delta H$  is the excess energy of the nanocrystalline sample in relation to its monocrystalline analog,  $V$  is the volume of the sample,  $\gamma_{TY}^*$  is the mean energy of triple joints determined as an excess over the energy of the grain boundaries converging to one line of their triple joint, and  $\lambda$  is the geometrical parameter equal to 2.63 for grains of random shape and size. For this case, integrating the relation

$$\frac{dD}{dt} = M \left( \frac{2\gamma_{GB}}{D} + \frac{\lambda\gamma_{TY}^*}{D^2} \right)$$

with respect to time at constant temperature, using the temperature dependence of the grain boundary mobility (2), and introducing designations for constants, we obtain

$$a_0(D^2 - D_0^2) - b_0(D - D_0) = k_0 t e^{-\frac{Q}{k_B T}}.$$

Here we have neglected the term proportional to  $\ln\left(\left(D - \frac{1}{2}\right) / \left(D_0 - \frac{1}{2}\right)\right)$  as it is much less in value than the other two terms for all mean grain sizes  $D$  under consideration.

Introducing the notation  $a = \frac{a_0}{k_0 t e^{-\frac{Q}{k_B T}}}$  and  $b = \frac{b_0}{k_0 t e^{-\frac{Q}{k_B T}}}$ , we obtain

$$a(D^2 - D_0^2) - b(D - D_0) = t. \quad (8)$$

The parameters  $a$  and  $b$  in relation (8) were optimized for each considered temperature proceeding from the requirement of the best reproduction of the data presented by dots in the plots given in Fig. 3.

The values  $Q_a$  and  $Q_b$  of the recrystallization activation energy  $Q$ , determined from the temperature dependences of  $a$  and  $b$ , respectively, were calculated by the least square method from the slope of the plots of  $\ln(a)$  and  $\ln(b)$  as functions of  $1/k_B T$  presented in Fig. 4. The temperature 1200 K was not considered in the calculation as it is higher than the temperature of the fcp-bcc polymorphic transformation of titanium (1156 K) [53]. In what follows the temperature 1200 K is considered only in qualitative testing of the results obtained in view of the necessary deviation of the data obtained for this temperature from the general trend observed for lower temperatures.

As can be seen from the calculation results (see Fig. 4), the values  $Q_a$  and  $Q_b$  of the recrystallization activation energy  $Q$  estimated from temperature dependences of  $a$  and  $b$  fit well to one another and are equal to 0.35 eV/atom to within the error of least square calculations.

Before proceeding to a discussion of the obtained simulation results and to their comparison to the available experimental data, we consider the description of these results by means of the empirical expression (6) often used to determine the quantitative characteristics of grain growth kinetics at constant temperature [52], including investigation of the grain growth process in the nanocrystalline titanium produced by forming a highly stressed state in a globe mill followed by primary recrystallization [54]. For doing this we take the logarithm of expression (6), having substituted for



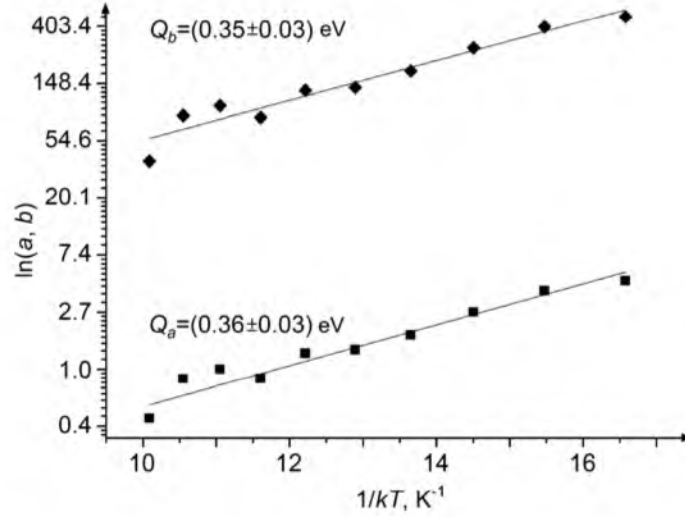


Fig. 4. Linear interpolation of the values of  $\ln(a)$  and  $\ln(b)$  calculated as functions of  $1/k_B T$  by the least square method.

the quantity  $c_1$  the expression showing its temperature dependence,  $c_1 = k_0 t e^{\frac{Q}{k_B T}}$ , and having introduced the notation  $y = 1/k_B T$ . As a result, we obtain the expression

$$\ln(D^n - D_0^n) + Q \cdot y - \ln(k_0) = \ln(t). \quad (9)$$

Considering  $n$ ,  $Q$ , and  $k_0$  in this expression as real parameters, we optimize them proceeding from the requirement of the best simultaneous reproduction of all data obtained by us for the temperatures from 700 to 1150 K. For comparison we perform the same optimization of the parameters of the following expression obtained in a similar way:

$$\ln(a_0(D^2 - D_0^2) - b_0(D - D_0)) + Q \cdot y = \ln(t), \quad (10)$$

which follows from relation (8) established by considering the contributions of grain boundaries and triple joints to the excess energy of a nanocrystalline material. For this case, the optimized parameters of relation (10) are  $a_0$ ,  $b_0$ , and  $Q$ . The determination of the mean grain sizes  $D$  depending on the natural logarithm of the simulation time for the temperatures under consideration and their interpolation by using the optimized parameters of expressions (9) and (10) is exemplified in Fig. 5 where the empirical relations (9) are presented by dashed curves and relations (10) by solid curves.

As can be seen from Fig. 5, the analytical expression (10), despite the lack of the exponent  $n$  among the parameters, describes the increase in mean grain size at constant temperature much better compared to the empirical relation (9), except for the temperature 1200 K, which was not considered in optimization and falls out from the general trend. From Fig. 3 it can be seen that relation (8) well describes the kinetics of grain growth at all temperatures considered. The deviations in the plots of Fig. 3 in the beginning of simulation at the lowest temperatures (700–800 K) are accounted for by that the molecular dynamic method failed to realize the steady-state recrystallization mode within the period of preparation of model samples at these temperatures. Therefore, it can be stated that the inclusion of the energy of triple joints allows one to describe well the kinetics of grain growth in nanocrystalline titanium by relation (8)

TABLE 1. Results of Calculations of Recrystallization Characteristics in Comparison with Available Experimental Data on Recrystallization of Nanocrystalline Titanium

Models	$Q$ , kJ/mol	$n$
Model 1. Independent interpolation for each temperature [Fig. 3, (8)]	$34 \pm 2$	2
Model 1. Interpolation by the relation general for all temperatures [Fig. 5, (9)]	$22.2 \pm 0.1$	2
Model 2. Interpolation by the relation general for all temperatures [Fig. 5, (10)]	$23.3 \pm 0.1$	$9.64 \pm 0.04$
Model 2. Experiment [54] for nanocrystalline titanium produced by intense deformation in a globe mill	128.3	11
	105.9	9
Experiment [55] for titanium produced by powder compaction	13	–
Other experiments on recrystallization for commercially pure titanium [56]	23, 35, 64, 66, 88	–

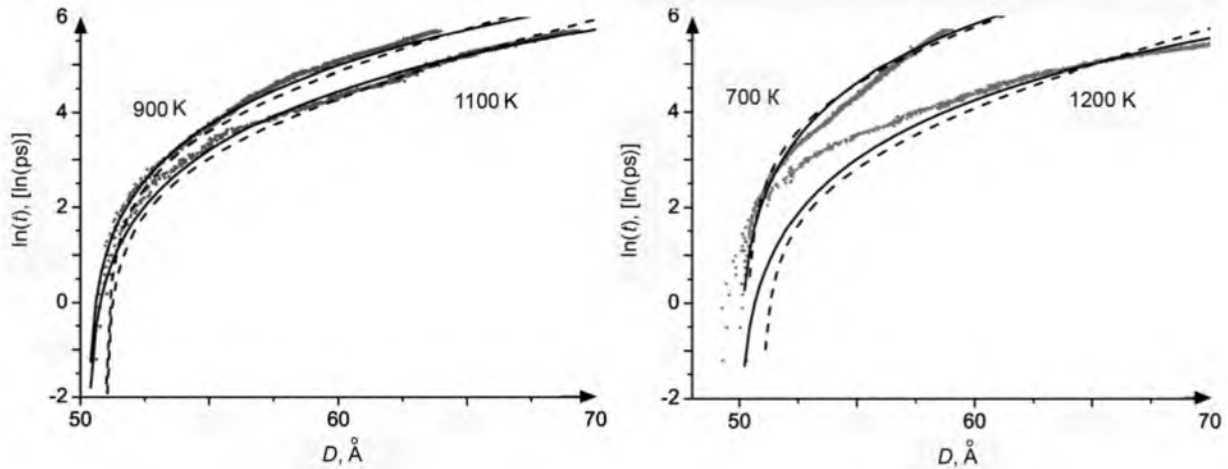


Fig. 5. Relationship between the mean grain size  $D$  and  $\ln(t)$  and the interpolation of this relationship by expression (9) (dashed curves) and by expression (10) (solid curves).

and, at the same time, it physically validates relation (8) in contrast to the empirical relation (6) for which the value of the exponent  $n$  is not substantiated (except for the simplest case  $n = 2$ ).

The final quantitative characteristics of the studied recrystallization of nanocrystalline titanium in comparison with available experimental data are presented in Table 1. In this table “Model 1” refers to our model taking into account triple joints where recrystallization is described with the use of the dependence of the mean grain sizes on the time of molecular dynamic simulation at constant temperature presented by expression (8) and its sequent (9). “Model 2” refers to a similar dependence presented by the well-known empirical expression (6) and its sequent (10). For the sake of comparison, the activation energy is expressed in terms of kJ/mol for all cases given in Table 1. The recrystallization exponent  $n$  is not given for the experiments in which it was not investigated, and only activation energy  $Q$  was used as a quantitative characteristic of recrystallization.

Let us discuss the data presented in Table 1. First we should note good consent between the value of the exponent  $n$  in the empirical expression (6) estimated from the simulation results ( $n = 9.64$ ) and the experimental data on the recrystallization of nanocrystalline titanium produced by deformation in a globe mill (value of  $n$ , according to Ref. 54, ranges from 9 to 11). The activation energy for recrystallization (128.3–105.9 kJ/mol) obtained in experiment [54] is much greater than that estimated from the data of simulation (23.3 kJ/mol for Model 2). It seems that this discrepancy can be qualitatively explained, for instance, by the saturation of titanium with nitrogen in the globe mill (increased nitrogen content in titanium subject to deformation in a globe mill is mentioned in Ref. 54). Inclusions of titanium nitride formed in this case segregate at grain boundaries in the course of their migration and reduce the mobility of grain boundaries with an increase in titanium grain size, increasing the effective activation energy for collective

recrystallization. However, the agreement between the values of the crystallization exponent  $n$  suggests that this characteristic is slightly sensitive to the grain-boundary segregation of nitrogen in fcp titanium when the empirical expression (6) is used to describe the grain growth kinetics. It should also be noted that, as can be seen from the data given in the second and third lines of Table 1, the calculated value of the activation energy slightly depends on whether the physically proved (Model 1) or empirical model (Model 2) is used.

The least recrystallization activation energy  $Q = 13$  kJ/mol in Table 1 refers to the submicroscopic titanium produced by powder compaction. This, rather low, value of  $Q$ , is probably related to the large excess volume of grain boundaries, which is typical for this production method.

From Table 1 it can also be seen that the activation energy values 22.2 and 34 kJ/mol obtained by the two methods are in the range of the lower values of the recrystallization activation energy for commercially pure titanium: 23, 35, 64, 66, and 88 kJ/mol. In view of the fact that the investigations were performed for perfectly pure titanium and that the effect of the atoms of residual impurities usually increases the activation energy for grain boundary migration, it can be concluded that the recrystallization activation energy for titanium without regard for the effect of impurities is 22–34 kJ/mol. It seems that for the temperature range 700–1150 K the activation energy cannot be determined more exactly, as it is sensitive to the method of determination. It is interesting that the activation energy obtained is much less than the activation energy for self-diffusion along random general-type grain boundaries in fcp titanium [ $82 \pm 6$  kJ/mol] that we have obtained from the simulation of the self-diffusion in nanocrystalline titanium with the use of the same potentials of interatomic interactions as in the present work. The corresponding method of calculation of the diffusion characteristics from the results of a molecular dynamic simulation is described elsewhere [57]. The calculated value is in good agreement with the experimental data on diffusion in nanocrystalline titanium (96 kJ/mol) [58]. A much lower value of the recrystallization activation energy compared to the self-diffusion activation energy for nanocrystalline titanium is also mentioned in Ref. 55. To elucidate the physical nature of this unusual proportion between the activation energies of recrystallization and grain-boundary self-diffusion calls for further investigation.

Thus, a physically substantiated description of the kinetics of grain growth during collective recrystallization which takes into consideration triple joints of grain boundaries has been given. Using a molecular-dynamic simulation of nanocrystalline titanium as an example, the kinetics of the collective recrystallization of titanium has been investigated and its activation energy has been determined in the context of a modified embedded atom method.

### **3. EXPERIMENTAL INVESTIGATION OF THE KINETICS OF COLLECTIVE RECRYSTALLIZATION OF NANOSTRUCTURED TITANIUM**

Investigation of the recrystallization kinetics for titanium in the initial nanostructured state upon annealings was performed for unalloyed titanium VT1-0 (chemical composition, wt. %: 0.010 Al – 0.004 C – 0.003 N – 0.120 Fe – 0.002 Si – 0.0008 H<sub>2</sub> – 0.143 O – base Ti).

In previous studies, modes for mechanical-thermal processing of alloy VT1-0 with the use of longitudinal and transverse-screw rolling have been developed that allow preparation of nanostructured titanium rods 4–10 mm in diameter according to TU 1825-001-02079230-2009 [59, 60]. In the present work we used 6-mm diameter rods that were subject to finishing annealing at a temperature of 623 K for 3 h to relieve internal stresses.

The growth of grains was studied for the temperature range 483–743 K. Structural examinations were performed for the cross-section longitudinal to the direction of rolling with the use of a Tecnai G2 F20 S-TWIN transmission electron microscope. The following methods of taking an image were used: light-field and dark-field images were obtained with transmission, including high-resolution, electron microscopy and light-field images were obtained with scanning electronic microscopy accompanied by detection of high-angle scattered electrons. Thin foils for transmission electron microscopy were prepared by mechanical grinding/polishing on a LaboPol-5 installation followed by jet polishing on a TenuPol-5 “Struers” installation with the use of a 20% HClO<sub>4</sub> + 80% CH<sub>3</sub>CO<sub>2</sub>H electrolyte.

The microstructure characteristics and mechanical properties of titanium in the initial NS state are given elsewhere [61]. It should be noted that the material structure contains in the main high-angle grain boundaries whose fracture makes about 76%. In the present work, to investigate the processes of collective recrystallization, the mean size

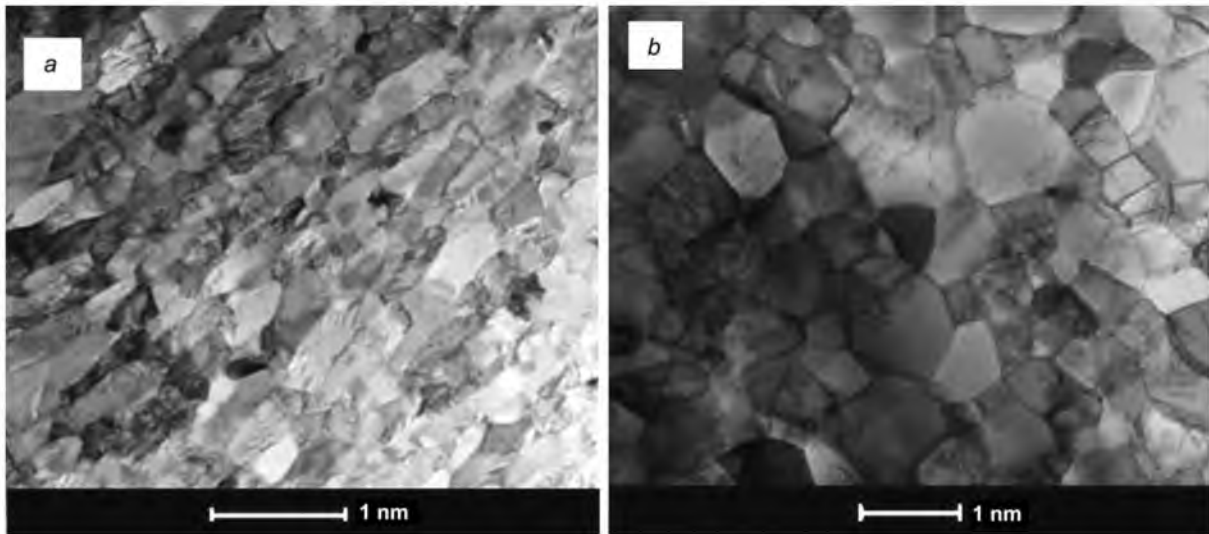


Fig. 6. Microstructure of titanium VT1-0 in the initial nanostructured state (a) and after 743 K, 1 h annealing (submicrocrystalline state) (b). Scanning transmission electron microscopy.

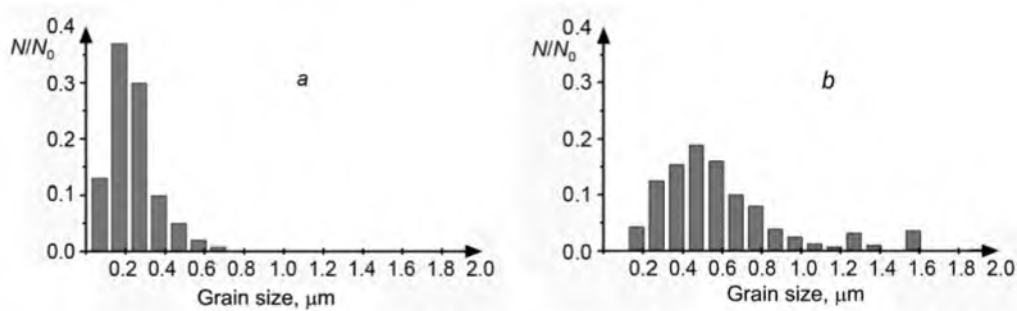


Fig. 7. Histogram of the subgrain size distribution for titanium VT1-0 in the initial nanostructured state (a) and after 743 K, 1 h annealing (submicrocrystalline state) (b).

of elements of the grain-subgrain structure was determined. For this purpose histograms of the subgrain size distribution over horizontal and vertical secants were constructed, and then averaging was performed. Thus, not only high-angle, but also low-angle boundaries have been taken into account.

The grain growth activation energy was determined from the temperature dependence of the kinetic parameter  $C$  in equation (6) (see Sec. 2). The linear approximation and the activation energy value were obtained by the least square method.

Figure 6 gives an image of the microstructure and Fig. 7 a histogram of the subgrain size distribution for titanium VT1-0 in the initial NS state and after annealing at 743 K. The temperature dependence of the kinetic parameter  $C$  from equation (6) in the approximation of the exponent  $n$  equal to 2 and 11 is given in Fig. 8. In the quadratic approximation of the grain growth, the temperature dependence of  $C$  can be subdivided into three sections which can be conventionally named “low-temperature”, “elevated-temperature”, and “high-temperature”.

For high annealing temperatures (above 743 K), abnormal grain growth is observed which is described by a bimodal grain size distribution (see Fig. 7b). The occurrence of the second maximum is related to the observed growth of individual coarse grains (see Fig. 6b). It is well known that one of the most often reasons for abnormal grain growth is the nonuniform distribution of the second phase particles that hinder migration of grain boundaries. However, in the case under consideration, another reason for this can be the presence of low-angle subgrain boundaries which

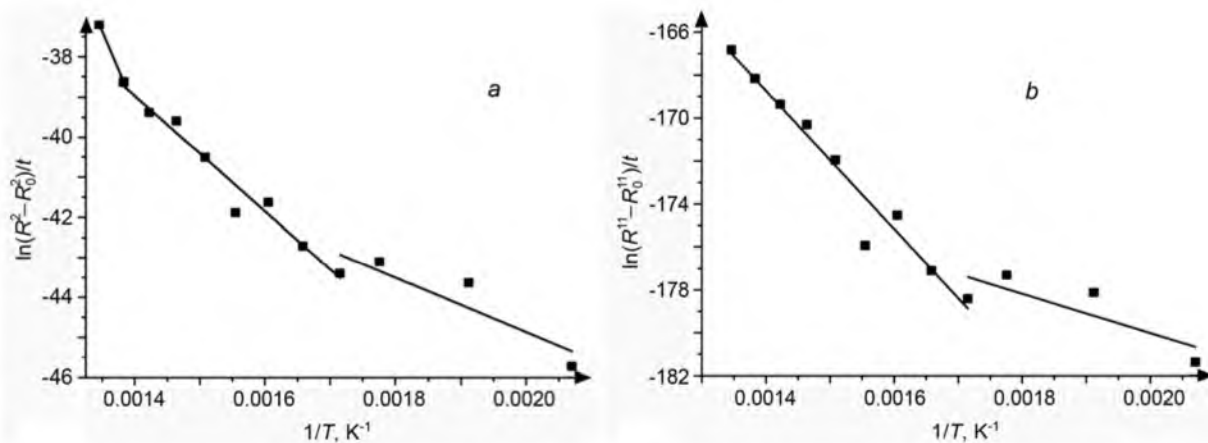


Fig. 8. Temperature dependence of the rate of grain growth in nanostructured titanium VT1-0 in the approximation of the exponent  $n = 2$  (a) and 11 (b).

substantially differ in mobility from high-angle boundaries. As a result, the grain growth kinetics is different: in this case, it should not obey a quadratic dependence of the grain size on time. In addition, the existence of two possible reasons for the abnormal growth of grains (subgrains) can introduce some indeterminacy in a comparison of experimental data with theoretical predictions.

At elevated temperatures (below 723 K but above 623 K) the grain growth can be considered normal; for this case, the activation energy determined from experimental data is  $(120 \pm 9)$  kJ/mol. The low-temperature range of grain growth is characterized by the activation energy  $(62 \pm 6)$  kJ/mol. It should be noted that in experiments on investigation of the grain growth in titanium, another kinetic dependence of the grain size on time was often observed after isothermal annealings (see, e.g., Ref. 54). Unfortunately, the spread in experimental data makes it impossible to determine exactly the parameter  $n$  in (6) for our experiments. However, the reasonability of the choice of the kinetic relation can be judged indirectly. Thus, if we use in calculations the kinetic relation with the exponent  $n$  equal to 11 (as in Ref. 54), the form of the temperature dependence of the kinetic factor  $C$  in equation (6) is retained; however, it appears to be broken only into two temperature intervals, and the grain growth activation energy is  $(270 \pm 20)$  kJ/mol at elevated temperatures and  $(80 \pm 40)$  kJ/mol at low temperatures (Fig. 8).

From the analysis performed it follows that at temperatures above 623 K (it should be noted that this is the temperature of preliminary annealing) several kinetic relations may describe the grain growth in titanium, and it is impossible to determine their form to within the experimental error (exactness of the estimation of the mean grain size related, in particular, to the homogeneity of the microstructure, inherited, in turn, from liquation distinctions in impurities in the titanium ingot). Nevertheless, the most probable is the classical kinetics with a quadratic dependence of the grain size on annealing time with activation energy of about 120 kJ/mol.

For low temperatures the kinetic dependence with  $n = 2$  and an activation energy of 62 kJ/mol shows the best convergence of data. Anyhow, irrespective of the choice of  $n$ , the experimentally determined grain growth activation energy cannot be over 80 kJ/mol at temperatures below 623 K. The activation energies for various processes in titanium taken from the literature and original data are given in Table 2.

It is well known that the kink in the temperature curve of recrystallization rate toward higher activation energies at higher temperatures is accounted for by the conventional activation of the migration of grain boundaries due to their breakaway from inclusions or segregates. Analysis of the data of Table 2 shows that at low temperatures the activation energy for collective recrystallization of NS titanium is close to the activation energy for grain-boundary self-diffusion (measured for the NS state [62]). The increase of the annealing temperature to 623 K and over results perhaps in breakaway of grain boundaries from hinder particles or segregates, and this effectively increases the process activation energy and causes abnormal growth of individual grains. The inclusions that hinder the motion of boundaries

TABLE 2. Values of the “Effective” Creep Activation Energy  $Q_c$  and Activation Energies for Collective Recrystallization,  $Q_{rec}$  (Original Data), Volumetric Self-Diffusion,  $Q_v$ , and Grain-Boundary Self-Diffusion,  $Q_b$ , for Titanium

$Q_c$ kJ/mol [62]		$Q_v$ kJ/mol [63]	$Q_b$ kJ/mol [63]	$Q_b^*$ kJ/mol [62]	$Q_{rec}$ kJ/mol	
SMC $T = 523-623$ K	CG	CG	CG	SMC	SMC $T < 623$ K	SMC $T > 623$ K
128	252	303	187	70	62	> 120

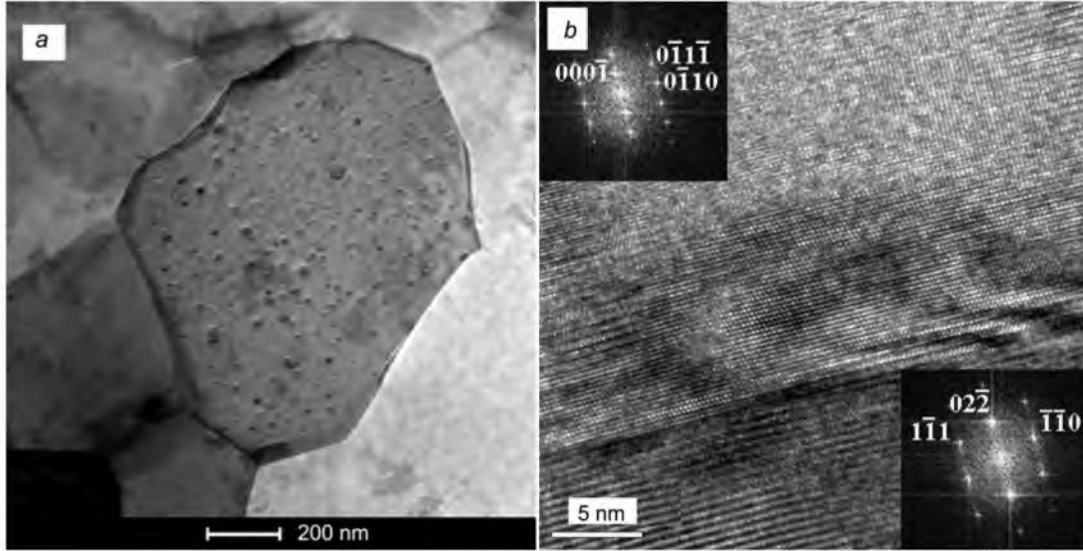


Fig. 9. Image of titanium carbide particles in NS titanium after annealing at 683 K: particles in a grain (scanning TEM) (a) and a single particle (b): the axis of the fcp matrix zone is  $[2\bar{1}\bar{1}0]$  and the axis of the fcc particle is  $[011]$  (high-resolution TEM with Fourier transformation of the image elements (top: from the matrix, bottom: from the particle)).

can be carbides, which should be present in the material in view of the low solubility of carbon in fcp titanium at low temperatures.

Actually, the existence of dispersed partially coherent carbides has been revealed in technically pure titanium (VT1-0) after various thermal treatments [64]. Fine-grained titanium carbides of lamellar morphology were also observed in our experiments on studying grain growth. Thus, after annealing of NS titanium at 683 K for 8 h, the grain bulk was filled with partially coherent inclusions (Fig. 9a). The particle material, as mentioned previously [64], were identified as carbide with an fcc sublattice of titanium atoms (Fig. 9b).

Other authors [65] related the stabilization of grain boundaries in NS titanium to grain-boundary segregation of carbon. The formation of carbon segregates was just detected in the material subject to annealing at 623 K. Thus, at temperatures over 623 K, grain boundaries can breakaway from carbon segregates and carbides can form in grain bulk (see Fig. 9).

According to the available experimental data [66, 67], the activation energy for bulk diffusion of carbon in fcp titanium ranges from 128 to 188 kJ/mol. Unfortunately, data on the grain-boundary diffusion of carbon in titanium are not available (most likely, the activation energy for the grain-boundary diffusion of carbon in titanium should be lower than that for bulk diffusion). Thus, the temperature dependence of grain growth in NS titanium can be controlled by

TABLE 3. Mechanical Properties of Titanium Alloys Used in Medicine

Properties	Grade-4*	VT1-0**	VT1-0 nanostructured state	VT6**
Ultimate strength, MPa	700	460	950	970
Plasticity, %	28	27	18	17

\*Manufacturer: Perryman Co, USA.

\*\*Manufacturer: Open Society “VSMPO-AVISMA Corp.”, RF.

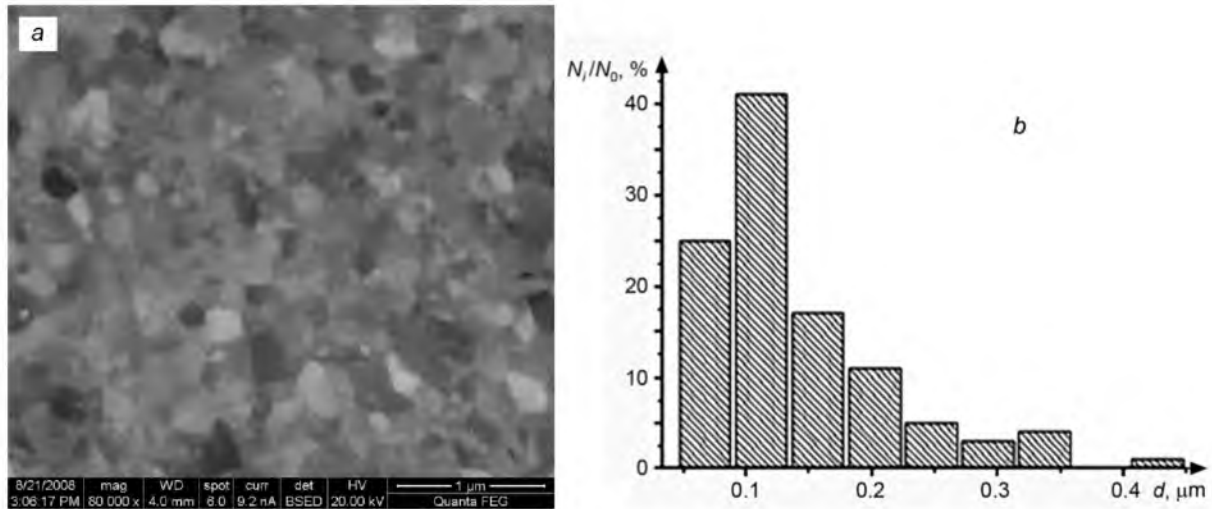


Fig. 10. Typical submicrocrystalline structure (*a*) and the grain size distribution histogram (*b*) for titanium VT1-0 processed by a combination of radial-shear, screw, and high-quality rollings:  $N_i$  is the number of grains of the  $i$ th range and  $N_0$  is the total number of grains.

both grain-boundary self-diffusion and grain-boundary (bulk) diffusion of carbon, depending on the mechanism of migration and its inhibition: by particles or by segregates.

#### 4. APPLICATION OF NANOSTRUCTURED TITANIUM IN MEDICINE

It is well known that, besides pure scientific problems of formation and stabilization of SMC structure and NS states in metal materials, there are problems of profitability and productivity of the methods of processing by plastic deformation, especially when it is necessary to produce batches of products of industrial assortment. One of examples is the production of SMC and NS unalloyed commercially pure titanium for medical uses.

However, notwithstanding that much work has been performed on the formation of submicrocrystalline and nanostructured states in titanium alloy VT1-0 by various methods, low-cost and high-efficiency production of alloy VT1-0 in SMC and NS states could be realized by using conventional methods of pressure processing of metals [36, 60, 61]. A combination of screw and high-quality rolling, previously adapted to rolling of hard-deformed tungsten-base and molybdenum-base alloys, has been used [68]. By using this method it became possible to produce a homogeneous globular submicrocrystalline structure with a mean grain size of  $\sim 150$  nm (Fig. 10) in small-diameter (6–8 mm) rods of commercially pure titanium (alloy VT1-0) with high-level mechanical properties (Table 3). The structure elements in this type of titanium vary in size, as a rule, between 0.05 and 0.5  $\mu\text{m}$  (nanosized grain fracture is  $\sim 35\%$ ).

The processing method using special deformation modes makes it possible to produce a more homogeneous nanostructure in which the element size range from 30 to 300 nm and the mean size is 90 nm (Fig. 11); the fraction of grains less than 100 in size makes 64%.

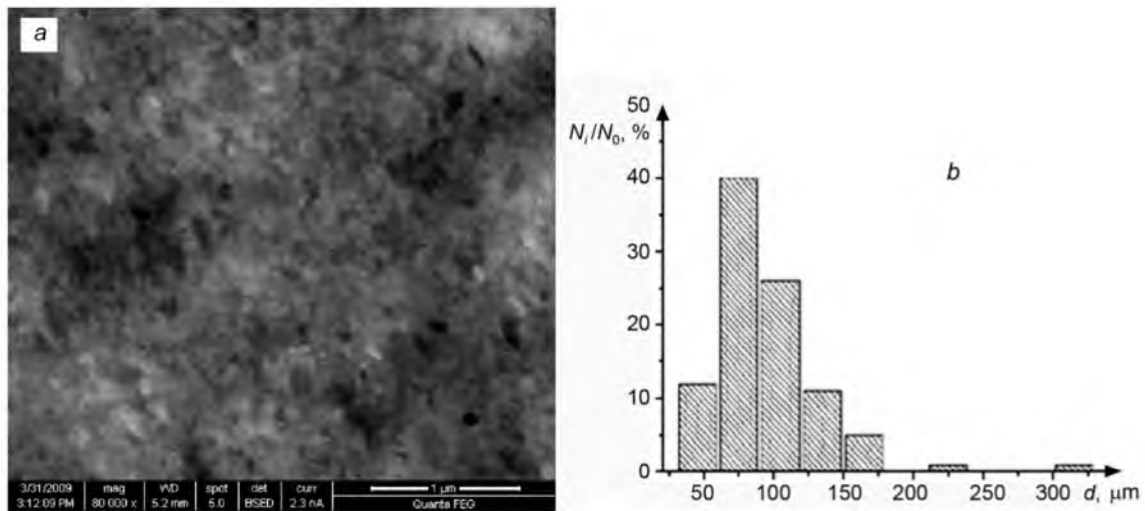


Fig. 11. Microstructure (*a*) and the grain size distribution histogram (*b*) for titanium VT1-0 processed by a combination of radial-shear, screw, and high-quality rollings under ultimate temperature-speed conditions:  $N_i$  is the number of grains of the  $i$ th range and  $N_0$  is the total number of grains.

The formation of SMC structure in titanium improves its tensile strength and ductility and increases the endurance limit under cyclic loading. The tensile ultimate strength of commercially pure titanium VT1-0 in the nanostructured state produced by a combination radial-shear, screw and high-quality rollings, as can be seen from Table 3, corresponds to the respective characteristics of titanium alloy VT6. The most interesting results have been obtained in torsional tests of screw implants intended for osteosynthesis. According to the test results, the screws made of NS alloy VT1-0 are highly competitive in strength with those made of alloy VT16 [36, 61] and also show extremely high plasticity (the maximum angle before torsional fracture is almost three times greater than that for alloy VT16). The structural plasticity of NS titanium is the most important reliability characteristic of screws made of this material, as under the conditions of actual medical prosthetic operation, fracture of screws made of a conventional titanium alloy may occur immediately in mounting. Previous low-cycle and high-cycle fatigue tests have shown that submicrocrystalline and nanostructured alloy VT1-0 shows fatigue resistance comparable to that of doped alloy VT6 [3, 36]. Recent experiments have shown that pure SMC titanium, including in notched samples, has rather high fatigue resistance [61]. The available data give all grounds to consider nanostructured titanium VT1-0 quite suitable to replace domestic alloys VT6 and VT16, and also foreign alloy Grade-4 applied in stomatology.

The low-cost and high-efficiency technological processes of production of structural shapes and round rods from nanostructured and submicrocrystalline titanium VT1-0 developed on the basis of the methods described above are used in industrial production of batches of materials for medical implants, which, as mentioned in Sec. 1, are delivered to clinics of the Russian Federation (Fig. 12).

The major problem in up-to-date medical materiology is the development of methods and technologies for surface modification of titanium and its alloys aimed at improving biocompatibility. The most currently widespread methods of surface processing of titanium, its alloys and other materials is deposition of thin protective bioinert oxide and bioactive calcium-phosphate coatings on a base material. Porous nanostructured calcium-phosphate coatings of rather large thickness (over 10  $\mu\text{m}$ ) on titanium and on its alloys are produced by the most technological and more and more often used microarc deposition method in calcium-phosphate-containing electrolytes in the form of water solutions or suspensions [70–73]. Implants made of SMC titanium alloys with bioactive ceramic coatings meet the requirements on resistance to fatigue failure, possess good osteointegration properties, and considerably reduce the bone tissue merging time [36]. Now work on the development of methods of deposition of calcium-phosphate coatings on SMC and NS titanium and on its alloys has been intensified [36, 73, 74] and methods of synthesis of nanocrystalline hydroxylapatite and electrolytes based on this substance have been developed [75, 76].



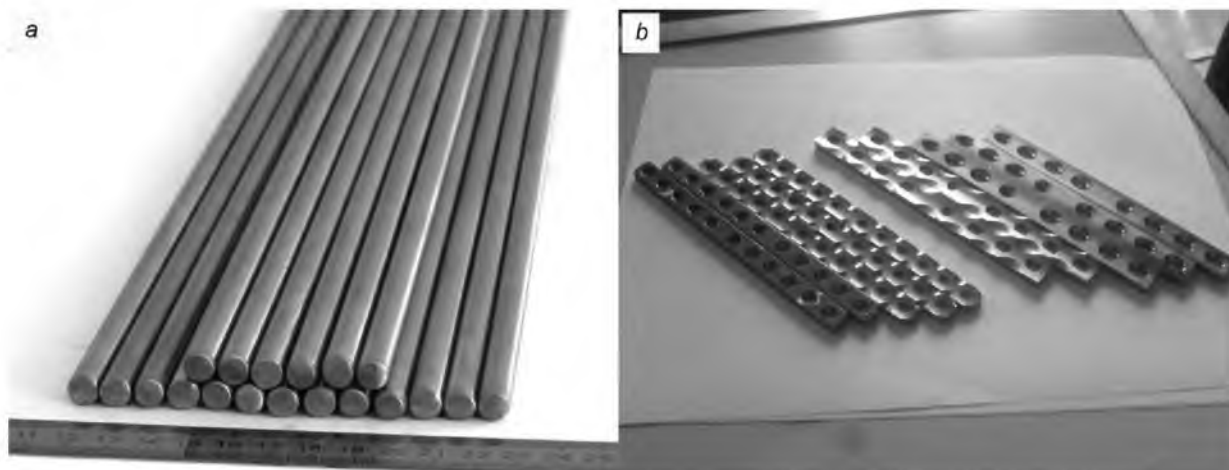


Fig. 12. Experimental batch of rods made of submicrocrystalline unalloyed titanium (alloy VT1-0) for manufacturing medical implants (a) and plates intended for use in traumatology made of submicrocrystalline unalloyed titanium (b).

## CONCLUSION

Analysis of the results of theoretical and experimental studies of the diffusion and diffusion-controlled processes in nanostructured metals produced by using intense plastic deformation has been performed.

The necessity of the account of grain boundary triple joints in a description of the kinetics of collective recrystallization of nanocrystalline materials has been physically substantiated.

The kinetics of collective recrystallization of titanium has been investigated and its activation energy has been found by the example of a molecular dynamic simulation of nanocrystalline titanium in the context of a modified embedded atom method. It has been shown that the increase of the mean grain size with simulation time at constant temperature is well described by an analytic relation that takes into account the contribution of grain-boundary triple joints to the thermodynamic force of the collective recrystallization process. The recrystallization activation energy is several times lower than the activation energy for the self-diffusion along random general-type grain boundaries in titanium.

It has been revealed that the temperature dependence of the collective recrystallization in SMC titanium has two pronounced intervals. At temperatures below the temperature of preliminary annealing of SMC titanium (chosen to be 623 K in the work under consideration), collective recrystallization (grain growth) obeys a power law with the exponent  $n = 2$  and the process activation energy is 62 kJ/mol. For annealing temperatures over 623 K the recrystallization activation energy is no less than 120 kJ/mol.

Problems of industrial production and practical implementation of nanostructured titanium as a material for medical implants have been discussed.

The work has been performed under Federal Purpose-Oriented Program “Scientific and Pedagogical Staff of Innovative Russia” for the years 2009–2013 (State contracts Nos. 02.740.11.0137 and 14.740.11.0022) with the use of the analytical equipment “Diagnostics of the structure and properties of nanomaterials” of Center of Shared Use of Research Equipment of Belgorod State University.

## REFERENCES

1. Yu. R. Kolobov, Diffusion-Controlled Processes at Grain Boundaries and Plasticity of Metallic Polycrystals [in Russian], Nauka, Novosibirsk (1998).

2. E. N. Kablov and E. R. Golubovskii, Thermal Stability of Nickel Alloys [in Russian], Mashinostroenie, Moscow (1998).
3. Yu. R. Kolobov, R. Z. Valiev, G. P. Grabovetskaya, *et al.*, Grain-Boundary Diffusion and Properties of Nanostructured Materials [in Russian], Nauka, Novosibirsk (2001).
4. R. E. Shalin, I. L. Svetlov, E. B. Kachanov, *et al.*, Monocrystals of High-Temperature Nickel Alloys [in Russian], Mashinostroenie, Moscow (1997).
5. E. N. Kablov, V. N. Toloraiya, and N. G. Orekhov, *Metalloved. Term. Obrab. Metallov*, **7**, 7–11 (2002).
6. A. N. Orlov, V. N. Perevezentsev, and V. V. Rybin, Grain Boundaries in Metals [in Russian], Metallurgia, Moscow (1980).
7. Yu. R. Kolobov, E. N. Kablov, E. V. Kozlov, *et al.*, Structure and Properties of Intermetallic Materials with Nanophase Hardening. [in Russian, ed. by E. N. Kablov and Yu. R. Kolobov], MISIS Publishers (2008).
8. M. I. Karpov, V. I. Vnukov, K. G. Volkov, *et al.*, *Materialoved.*, No. 2, 47–52 (2004).
9. M. V. Alfimov, *Ros. Nanotekhnol.*, **2**, No. 7/8, 1–5 (2007).
10. Yu. R. Kolobov, E. F. Dudarev, T. G. Lengdon, *et al.*, *Metally*, No. 2, 116–122 (2004).
11. E. V. Naidenkin, E. F. Dudarev, Yu. R. Kolobov, *et al.*, *Mater. Sci. Forum*, **503/504**, 983–988 (2006).
12. V. N. Perevezentsev, *Fiz. Met. Metalloved.*, **83**, Issue 2, (1997).
13. G. P. Grabovetskaya, I. P. Mishin, I. V. Ratochka, *et al.*, *Pis'ma Zh. Tekh. Fiz.*, **34**, No. 4, 1–7 (2008).
14. Yu. R. Kolobov, G. P. Grabovetskaya, M. B. Ivanov, *et al.*, *Scripta Met.*, **44**, 873–878 (2001).
15. R. Wurschum and K. Reimann, S. Grub, *et al.*, *Phil. Mag. B*, **76**, 407 (1997).
16. Yu. R. Kolobov, A. G. Lipnitskii, I. V. Nelasov, and G. P. Grabovetskaya, *Izv. Vyssh. Uchebn. Zaved., Fiz.*, No. 4, 47–60 (2008).
17. Yu. R. Kolobov and K.V. Ivanov, *Mater. Sci. Forum*, **503/504**, 141–148 (2006).
18. G. P. Grabovetskaya, I. V. Ratochka, Yu. R. Kolobov, and L. N. Puchkareva, *Fiz. Met. Metalloved.*, **83**, No. 3, 112–116 (1997).
19. V. N. Perevezentsev, A. S. Pupylin, Yu. V. Svirins, *Ibid.*, **100**, No. 1, 17–23 (2005).
20. Yu. R. Kolobov, G. P. Grabovetskaya, I. V. Ratochka, *et al.*, *Ann. Chim.*, No. 11, 483–492 (1996).
21. Yu. R. Kolobov, G. P. Grabovetskaya, K. V. Ivanov, and M. B. Ivanov, *Inter. Sci.*, **10**, No. 1, 31–36 (2002).
22. J. Ribbe, D. Baiter, G. Scmitz, and S. Divinski, *Scripta Mat.*, **61**, No. 2, 129–132 (2009).
23. V. I. Betekhtin, V. Sklenicka, I. Saxl, *et al.*, *Fiz. Tverd. Tela*, **52**, 1517–1523 (2010).
24. R. Lapovok, D. Tomus, J. Mang, *et al.*, *Acta Mater.*, **57**, 2909–2918 (2009).
25. S. V. Divinski, J. Ribbe, G. Reglitz, *et al.*, *J. Appl. Phys.*, **106**, 063502–063508 (2009).
26. V. I. Betehtin, Yu. R. Kolobov, B. K. Kardashev, *et al.*, in: Proc. the 51st Intern. Conf. “Topical Problems of Strength”, Kharkov, Ukraine, May 16–20, 2011 [in Russian], Kharkov (2011), p. 12.
27. M. B. Ivanov, A. V. Penkin, Yu. R. Kolobov, *et al.*, *Deform. Razrush. Mater.*, No. 9, 13–18 (2010).
28. H. Gleiter, *Prog. Mater. Sci.*, **33**, 223–315 (1989).
29. C. E. Krill, L. Helfen, D. Michels, *et al.*, *Phys. Rev. Lett.*, **86**, 842–845 (2001).
30. A. Caro and H. Van Swygenhoven, *Phys. Rev.*, **B63**, 134101 (2001).
31. J. Weissmüller, in: Proc. the 22nd Riso Intern. Symp. on Materials Science: Structure, Properties and Modelling, Denmark (2001), pp. 155–176.
32. Physical Mesomechanics and Computer Construction of Materials [in Russian, ed. by V. E. Panin], Nauka, Novosibirsk (1995).
33. R. Z. Valiev and I. V. Aleksandrov, Bulk Nanostructured Materials: Production, Structure and Properties [in Russian], Akademkniga, Moscow (2007).
34. Yu. R. Kolobov, M. B. Ivanov, E. V. Golosov, and A. V. Penkin, Method of Production of Submicrocrystalline Structure in Unalloyed Titanium [in Russian], RUC1 Patent No. 2389568, in: *Izobretenia. Poleznye Modeli. Bul.* No. 14, 20.05.2010.
35. Yu. R. Kolobov, I. V. Ratochka, K. V. Ivanov, and A. G. Lipnitskii, *Izv. Vyssh. Uchebn. Zaved., Fiz.*, No. 8, 49–64 (2004).
36. Yu. R. Kolobov, *Rus. Nanotekh.*, **4**, No. 11/12, 69–81 (2009).
37. H. Gleiter, *Acta Mater.*, **48**, 1–29 (2000).

38. K. S. Kumar, H. van Swygenhoven, and S. Suresh, *Ibid.*, **51**, 5743–5774 (2003).
39. H. Gleiter, *Prog. Mater. Sci.*, **33**, 223–330 (1989).
40. K. Lu and N. X. Sun, *Philosoph. Magazine Lett.*, **75**, No. 6, 389–395 (1997).
41. R. A. Andrievski, *J. Mater. Sci.*, **38**, 1367–1375 (2003).
42. J. Weissmuller, *Nanostruct. Mater.*, **3**, No. 1/6, 261–273 (1993).
43. C. A. Detor and J. Schuh, *Acta Mater.*, **55**, 4221–4232 (2007).
44. J. Detor, M. K. Miller, and C. A. Schuh, *Philosoph. Magazine*, **86**, 4459–4475 (2006).
45. R. G. Hennig, T. J. Lenosky, D. R. Trinkle, *et al.*, *Phys. Rev. B*, **B78**, 054121 (2008).
46. W. Kohn and L. J. Sham, *Phys. Rev.*, **A140**, 1133–1138 (1965).
47. D. Moldovan, V. Yamakov, D. Wolf, and S. R. Phillpot, *Phys. Rev. Lett.*, **89**, 206101–206105 (2002).
48. D. Farkas, E. Bringa, and A. Caro, *Phys. Rev.*, **B75**, 184111 (2007).
49. W. G. Hoover, *Phys. Rev. A*, **31**, 1695–1697 (1985).
50. A. G. Lipnitskii, *Materialoved.*, No. 2, 2–9 (2009).
51. S. S. Gorelik, *Recrystallization of Metals and Alloys* [in Russian], Metallurgia, Moscow (1978).
52. M. Hatherly and F. Humphreys, *Recrystallization and Related Annealing Phenomena*. Pergamon (2004).
53. U. Zwicker, *Titan und Titanlegierungen*, Springer, Berlin (1974).
54. F. Sun, A. Zuniga, P. Rojas, and E. J. Lavernia, *Metallurg. Mater. Trans. A*, **37**, 2069–2078 (2006).
55. S. H. Zahiri, D. Fraser, and M. Jahedi, *J. Thermal Spray Technol.*, **18**, No. 1, 16–22 (2009).
56. F. M. Guclu, H. Cimenoglu, and E. S. Kayal, *Mater. Sci. Eng. C*, **26**, 1367–1372 (2006).
57. A. G. Lipnitskii, I. V. Nelasov, and Yu. R. Kolobov, *Defect and Diffusion Forum*, **309/310**, 45–51 (2011).
58. E. F. Dudarev, G. P. Pochivalova, Yu. R. Kolobov, *et al.*, *Rus. Phys. J.*, **47**, 617–625 (2004).
59. Yu. R. Kolobov, M. B. Ivanov, E. V. Golosov, and A. V. Penkin, *Method of Production of Submicrocrystalline Structure in Unalloyed Titanium* [in Russian], RF Patent No. 2389568, 29.12.2008.
60. M. B. Ivanov, A. V. Penkin, Yu. R. Kolobov, *et al.*, *Deform. Razrush. Mater.*, No. 9, 13–18 (2010).
61. Ivanov M.B., Yu. R. Kolobov, E. V. Golosov, *et al.*, *Rus. Nanotekh.*, **6**, No. 5/6, 72–78 (2011).
62. G. P. Grabovetskaya, Yu. R. Kolobov, L. V. Chernova, and N. V. Girsova, *Fiz. Mezomekh.*, **5**, No. 6, 87–94 (2002).
63. Chr. Herzig, T. Wilger, T. Przeorski, *et al.*, *Intermetallics*, No. 9, 431–442 (2001).
64. D. A. Nechaenko, S. S. Manohin, and M. B. Ivanov, in *Proc. XI Ural School-Seminar of Young Metal Scientists*, November 8–12, 2010, Ekaterinburg (2010), pp. 158–161.
65. I. Semenova, G. Salimgareeva, G. Da Costa, *et al.*, *Adv. Eng. Mater.*, **12**, 803–807 (2010).
66. S. Suzuki, T. Sato, A. Kurokawa, and S. Ichimura, *J. Surf. Anal.*, **12**, 166–169 (2005).
67. C. Arvieu, J. P. Manaud, and J. M. Quenisset, *J. All. Comp.*, **368**, 116–122 (2004).
68. A. N. Shapoval, S. M. Gorbatyuk, and A. A. Shapoval, *Intense Pressure Processing of Tungsten and Molybdenum* [in Russian], “Ruda I Metally” Publishing Hous, Moscow (2006).
69. R. Z. Valiev, I. P. Semenova, V. V. Latysh, *et al.*, *Nanotechnol. Rus.*, **3**, No. 9/10, 593–601 (2008).
70. Yu. R. Kolobov, A. V. Karlov, L. S. Bushnev, and E. E. Sagimbaev, *Acta Orthoped. Scand.*, **69**, No. 280, 48–50 (1998).
71. A. V. Karlov, Yu. R. Kolobov, L. S. Busnev, *et al.*, *Med. Biolog. Engin. Comp.*, **37**, No. 3, 198–199 (1999).
72. Yu. R. Kolobov, A. V. Karlov, E. E. Sagymbaev, *et al.*, *Bioceramics*, **13**, 215–218 (2000).
73. Yu. R. Kolobov, O. A. Druchinina, M. B. Ivanov, *et al.*, *Nano-Mikrosistem. Tekh.*, No. 2, 48–54 (2009).
74. G. A. Shashkina, M. B. Ivanov, E. V. Legostaeva, *et al.*, *Fiz. Mezomekh.*, **7**, Pt. 2, 123–126 (2004).
75. N. N. Volkovnyak, M. B. Ivanov, Yu. R. Kolobov, A. A. Buzov, and V. P. Chuev, *Method of Production of Nanosized Hydroxylapatite* [in Russian], RF Patent No. 2342319, 28.12.2008.
76. N. N. Volkovnyak, M. B. Ivanov, Yu. R. Kolobov, *Method of Production of Electrolyte for Deposition of Bioactive Coatings* [in Russian], RF Patent No. 2345181, 27.01.2009.